WIND LOADS ON ROOFING SYSTEM AND PHOTOVOLTAIC SYSTEM INSTALLED PARALLEL TO FLAT ROOF

TETSUO YAMBE[1], YASUSHI UEMATSU[2], and KOSUKE SATO[1]

[1]*Graduate School of Engineering, Tohoku University, Sendai, Japan*
[2]*National Institute of Technology (KOSEN), Akita College, Akita, Japan*

Mechanically-attached waterproofing system has become popular in Japan. Being vulnerable to wind actions, especially to suctions, this roofing system is often damaged by strong winds. Similarly, photovoltaic (PV) systems installed on flat roofs are often damaged by strong winds, because the PV panels are subjected to large wind forces in an adverse wind. In order to reduce such damage to both systems, the authors propose to install the PV panels parallel to the flat roof with gaps between them, which may reduce the net wind forces on the PV panels due to the effect of pressure equalization. In addition, the wind pressures acting on the waterproofing system will decrease significantly. The present paper investigates the validity of the above-mentioned idea. The wind pressures underneath the PV panels, called 'layer pressures', are evaluated by a numerical simulation using the unsteady Bernoulli equation together with the time history of external pressures measured at many locations on the rooftop of a flat-roofed building model in a turbulent boundary layer. The results clearly indicate a significant reduction of wind forces acting on the PV panels as well as on the waterproofing system. The use of PV panels for reducing the wind pressures on waterproofing system is quite effective to the corner region of the roof, where very large suctions are induced in a diagonal wind.

Keywords: Mechanically-attached waterproofing system, Pressure equalization, Wind tunnel experiment, Numerical simulation, Unsteady Bernoulli equation.

1 INTRODUCTION

Mechanically-attached waterproofing system is often used for flat roofs, because the amount of organic solvent used is so small that it is friendly to the environment. However, it is vulnerable to wind actions and often damaged by strong winds. Photovoltaic (PV) systems installed on flat roofs have become popular in Japan. The PV panels are usually installed at an angle of 20° - 30° against the roof surface, considering higher power generation efficiency. In such a case panels are subjected to large wind forces in an adverse wind and often damaged by strong winds.

The present paper proposes to install the PV panels parallel to the flat roof with small gaps between them. Figure 1 shows a schematic of the wind forces acting on the waterproofing system without and with PV panels. Without PV panels the waterproofing system is subjected to large suctions directly. With PV panels, on the other hand, it is subjected to the pressure of the space between roof surface and PV panels (called 'layer pressure', hereafter). The gap between PV panels may produce a kind of pressure equalization to the space between the panels and roof surface, resulting in a reduction of wind pressures on the waterproofing system. The net wind force acting

on the PV panel, provided by the difference between wind pressures on the top and bottom surfaces of the panel, is expected to be much smaller than that for the regular case where the panels are installed at an angle of $20° – 30°$ against the roof surface.

(a) Without PV panels   (b) With PV panels
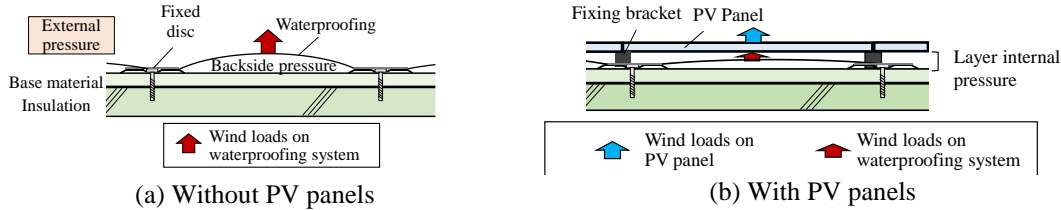
Figure 1. Wind loads on waterproofing system and PV panels.

It is necessary for investigating the wind loads on PV panels and waterproofing system to evaluate the layer pressure precisely. The authors apply a numerical simulation to this subject, because it is quite difficult, almost impossible, to measure the pressure directly in the wind tunnel experiment with a small model at a geometric scale of 1/100 to 1/200. Note that the distance between roof and PV panels is only several centimeters at full scale. The layer pressure is simulated by using the unsteady Bernoulli equation together with the time history of external pressures measured at many locations on the rooftop of a building model in a wind tunnel.

2   WIND TUNNEL EXPERIMENT

2.1   Experimental Procedures

The experiment was carried out in an Eiffel type wind tunnel at the Department of Architecture and Building Science, Tohoku University, which has a working section of 1.4 m width, 1.0 m height and 6.5 m length. A turbulent boundary layer with a power law exponent of approximately 0.21 is generated in the wind tunnel using spires and roughness blocks. The turbulence intensity of the flow at a height of 100 mm (building model height) is approximately 0.15. This flow roughly corresponds to natural winds over typical suburban terrain.

Figure 2 shows the experimental model and pressure tap location. The present study focuses on a flat-roofed three-story residential house. The roof height H is 10 m and the parapet height h_p is 150 mm or 300 mm. Parapet thickness is 150 mm. The geometric scale of this wind tunnel model is assumed 1/100. The design wind speed U_H at the roof height H is calculated based on the AIJ (2015) which is about Recommendations for Loads on Buildings. It is assumed that the 'basic wind speed' is 35 m/s and the Terrain Category is III (suburban exposure). As a result, the design wind speed U_H is calculated as 27.8 m/s. The wind speed at the model height is set to 8 m/s in the wind tunnel experiment. The velocity scale of the wind tunnel experiment is therefore 1/3.5, resulting in a time scale of 1/28.8. The wind angle θ is changed from $0°$ to $45°$ at a step of $5°$ (see Figure 2b). Wind pressures at all pressure taps are measured simultaneously with a sampling frequency of 800 Hz during a period of approximately 21 s, which corresponds to 600 s at full scale. The measurement is repeated 10 times under the same condition. The distortion of the measured fluctuating pressures due to tubing is compensated in the frequency domain by using the frequency response function of the tubing system. The wind pressure coefficient C_{pe} is defined in terms of the dynamic pressure q_H of the approach flow at the model height H. The statistical values of C_{pe} are evaluated by applying ensemble average to the results of 10 runs. The most critical minimum pressure coefficient irrespective of wind direction and tap location is represented by $C_{pe,min}$ in the present paper.
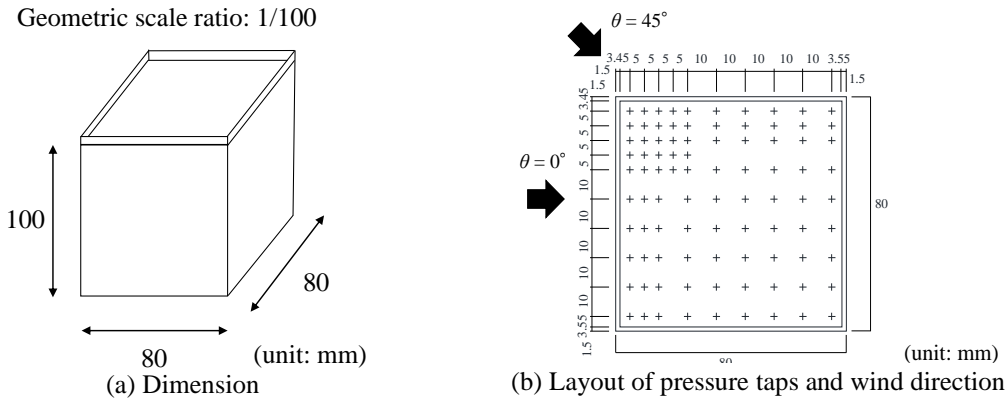
Geometric scale ratio: 1/100

(a) Dimension

(b) Layout of pressure taps and wind direction

Figure 2. Wind tunnel model and pressure tap location.

2.2 Wind Pressure Distribution on the Roof

Large suctions are induced near the windward corner due to the generation of conical vortices in diagonal winds. The value of $C_{pe,min}$ was −4.8 at $\theta = 35°$ when $h_p = 15$ cm, while it is −4.6 at $\theta = 40°$ when $h_p = 30$ cm. As the parapet height increases, the magnitude of $C_{pe,min}$ decreases, while the area of relatively large suction increases. This is because the distance of conical vortices from the roof surface increases with an increase in h_p.

3   SIMULATION OF WIND PRESSURES ON PV PANELS AND WATER PROOFING SYSTEM

3.1   Coefficient of Clearance for the Gap Between PV Panels

In the simulation of layer pressures underneath the PV panels, it is necessary to evaluate the shape resistant coefficient C_L and the discharge coefficient k_e for the gap between PV panels, as will be described below. The values of these parameters were experimentally obtained by using a full-scale specimen of the gap. In practice, the specimen was attached to the pressure chamber of a dynamic loading apparatus (see Gavanski *et al.* 2015) with the upper side of PV panels facing the pressure chamber. A Pressure Loading Actuator (PLA) generated pressure fluctuations inside the chamber by using a time history of wind pressure coefficient obtained from the above-mentioned wind tunnel experiment. There was a small space on the opposite side of the specimen and the internal pressure of this space was measured by a pressure transducer. The internal pressure was also numerically simulated by changing the values of C_L and k_e. The optimum values of C_L and k_e, with which the numerical result agreed well with the experimental one, were determined by trial and error; that is, $C_L = 1.42$ and $k_e = 0.55$. Note that the equivalent width D_e of the gap was assumed 3 mm, considering the practical configuration of the gap.

3.2   Methods of Simulation

The space underneath the PV panels are divided into several virtual sub-spaces, which are called 'rooms' in the present paper. The unsteady Bernoulli equations for the gap flows in the x, y and z directions are given by Eqs. (1) – (3) (Kopp *et al.* 2010). Note that x and z represent the horizontal directions and y the vertical direction.

$$\frac{\rho l_{\iota,j}\dot{U}_{i,j+1}}{q_H} = C_{i,j} - C_{i,j+1} - \frac{1}{2q_H}C_L\rho_{i,j}U_{i,j+1}\big|_{i,j}U_{i,j+1}\big| - \frac{\Delta p_x}{q_H} \qquad (1)$$

$$\frac{\rho l_e\ddot{U}_{i,j}}{q_H} = C_{i,j} - {}_eC_{i,j} - \frac{1}{2q_H}C_{Le}\rho\,{}_eU_{i,j}\big|\,{}_eU_{i,j}\big| - \frac{\Delta p_e}{q_H} \qquad (2)$$

$$\frac{\rho l_{\iota,j}\dot{U}_{i,j+1}}{q_H} = C_{i,j} - C_{i,j+1} - \frac{1}{2q_H}C_L\rho_{i,j}U_{i,j+1}\big|_{i,j}U_{i,j+1}\big| - \frac{\Delta p_z}{q_H} \qquad (3)$$

where subscript (i, j) represents the room location in a matrix form; subscript 'e' represents the external space or pressure; U = gap flow speed (m/s); q_H = dynamic pressure (N/m^2); ρ = air density (kg/m^3); l = gap depth (m); $_eC$ = external pressure coefficient; C = layer pressure coefficient; C_L = shape resistance coefficient in the horizontal direction; C_{Le} = shape resistance coefficient in the vertical direction; and Δp = pressure loss (N/m^2). The external pressure coefficients at the location of gaps between PV panels are obtained from the experimental data to which a spatial interpolation with a Spline function of the third order is applied. Considering the calculation load, the above equations are solved by the Runge-kutta method. The internal pressure P in each room can be obtained by the following Eq. (4):

$$\frac{dP}{dt} = \frac{\gamma P_0}{V_0}\sum Q \qquad (4)$$

where γ = heat capacity ratio; P_0 = atmospheric pressure (N/m^2); V_0 = virtual room volume (m^3); and Q = flow rate (m³/s). The layer pressure at the next step is calculated by the Euler method with a very small time step.

3.3   Location of PV Panels on the Roof and Virtual Room Division

Figure 3 shows the location of PV panels and the definition of virtual rooms. Focus is on two locations of the PV panels; one is near the windward corner where large suctions are induced by conical vortices, and the other is near the roof center where PV panels are usually installed in practice. The wind force (or net wind pressure) coefficient C_f on the PV panel is provided by the difference between the external pressure coefficient C_{pe} obtained from the wind tunnel experiment and the layer pressure coefficient C_{pi} obtained from the simulation. The net wind force coefficient $C_{f,panel}$ of each panel is provided by the spatial average of C_f over the whole panel area. The maximum peak value of $C_{f,panel}$ is obtained from the time history of $C_{f,panel}$.

4   RESULTS

4.1   Wind Loads on PV Panels and a Comparison with the Specification of JIS

In the case where the PV panels are installed near the roof corner, the maximum peak value of $C_{f,panel}$ was found to be -1.2 on Panel 5 at $\theta = 35°$. In the case where the PV arrays are installed near the roof center, on the other hand, it was found to be -1.0 on Panel 5 at $\theta = 35°$.

JIS C 8955 (2017) provides wind force coefficients on PV panels. The value for $\beta = 0°$ is specified as -0.6. Note that the wind force coefficient is 'equivalent static wind load'; i.e., peak wind force coefficient divided by a gust effect factor. Therefore, the present results for the peak wind force coefficients can be compared with the JIS specification multiplied by the gust effect factor. In the case of $H = 10$ m for Terrain Category III the gust effect factor is specified as 2.5.

Thus the peak wind force coefficient is estimated as -1.5 ($= -0.6 \times 2.5$), which is larger in magnitude than the maximum value of $C_{\text{f,panel}}$ obtained above ($= -1.0$).
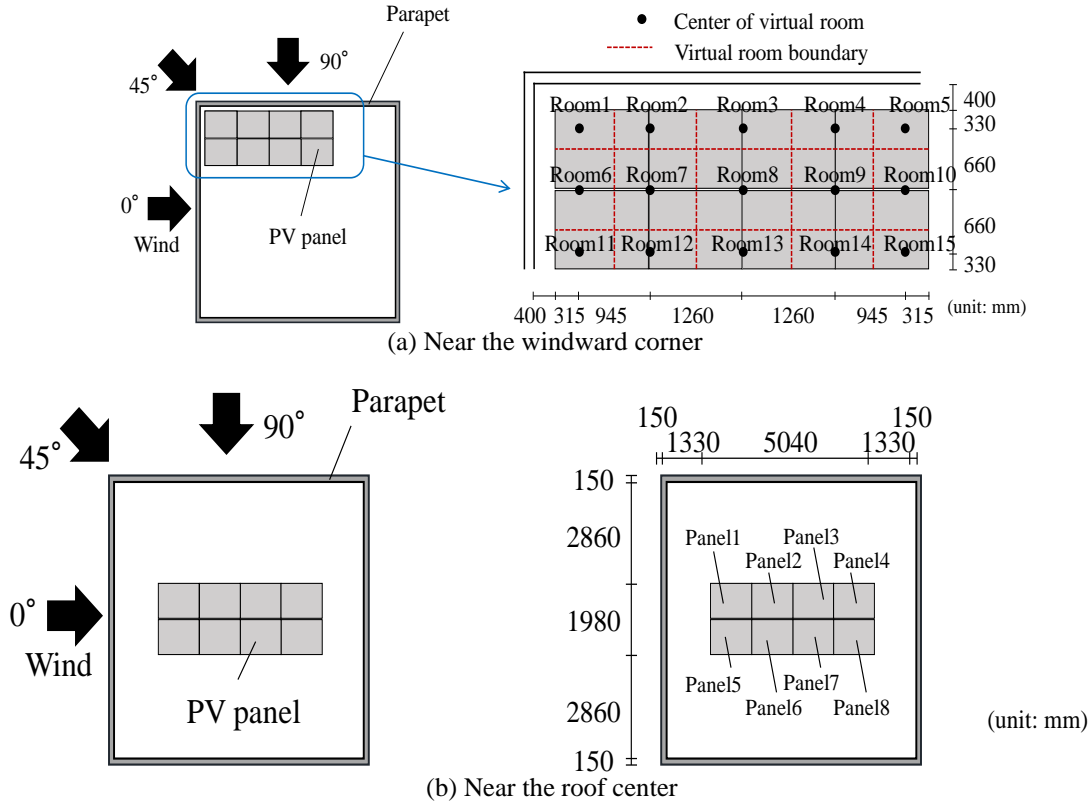
Figure 3. Location of PV panels and definition of virtual room and panel number.

4.2 Wind Loads on Waterproofing System

For the purpose of simplicity, it is assumed that the wind pressure underneath the waterproofing sheet is zero. In this case, the net wind pressure acting on the waterproofing sheet is given by the wind pressure on the top surface of the sheet. Figure 4 shows the most critical values of the minimum peak external and layer pressure coefficients, $\check{C}_{pe}$ and $\check{C}_{pi}$, irrespective of wind direction for each virtual room when hp = 15 cm and 30 cm. Without PV panels the waterproofing system is subjected to the external pressures represented by the circles. With PV panels, on the other hand, it is subjected to the layer pressures represented by the squares. It is found that the value of $\check{C}_{pi}$ is generally smaller in magnitude than that of $\check{C}_{pe}$. In particular, the difference is fairly large for the panels located near the roof corner. This feature indicates that the wind loads on the waterproofing system are significantly reduced by installing the PV panels with gaps between them above the waterproofing system.
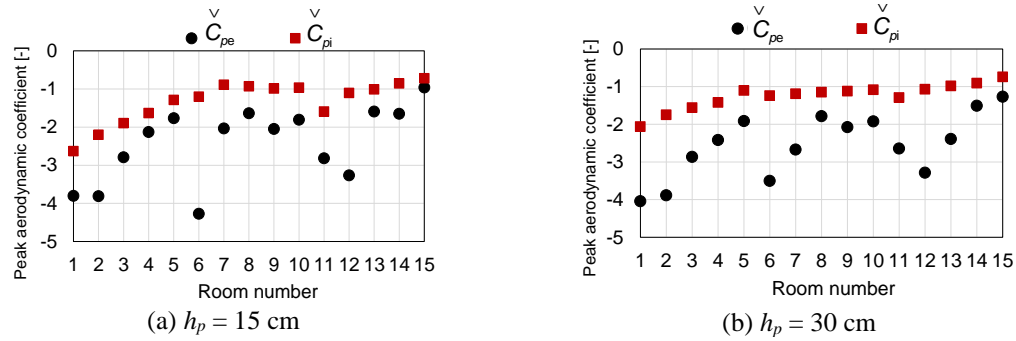
Figure 4. Most critical values of the minimum peak external and layer pressure coefficients irrespective wind direction.

5   CONCLUDING REMARKS

The present study has proposed to install PV panels parallel to the flat roof with small gaps between them. The effect of this method on the wind load reduction on both the PV panels and the waterproofing system was investigated based on a wind tunnel experiment of external pressures and a numerical simulation of layer pressures (pressures underneath the PV panels). The results clearly indicate that this method is quite effective, resulting in an improvement of wind resistance of both the PV system and the waterproofing system.

References

AIJ, *Recommendations for Loads on Buildings*, Architectural Institute of Japan, 2015.

Gavanski, E., Takahashi, M., Uematsu, Y., and J. Morrison, M., *Quantitative Performance Evaluation of Time-Varying Wind Pressure Loading Actuator,* AIJ Journal of Technology and Design, 21(49), 1075–1080, October, 2015.

Kopp, G. A., Morrison, M. J., Gavanski, E., Henderson, D. J., and Hong, H. P., *"Three Little Pigs" Project: Hurricane Risk Mitigation by Integrated Wind Tunnel and Full-Scale Laboratory Tests,* Natural Hazards Review, 11(4), 151–161, November, 2010.

JIS C 8955, *Load Design Guide on Structure for Photovoltaic Array,* Japanese Standards Association, Japan, 2017.